Numerical behavior for quasi static thermoelasticity without positive definite elasticity

J. BALDONEDO[1)], J. R. FERNÁNDEZ[2)], R. QUINTANILLA[3)]

[1)] *CINTECX, Departamento de Ingeniería Mecánica, Universidade de Vigo,*
Campus As Lagoas Marcosende s/n, 36310 Vigo, Spain,
e-mail: jacobo.gonzalez.baldonedo@uvigo.es

[2)] *Departamento de Matemática Aplicada I, Universidade de Vigo,*
ETSI Telecomunicación, Campus As Lagoas Marcosende s/n, 36310 Vigo, Spain,
e-mail: jose.fernandez@uvigo.es

[3)] *Departamento de Matemáticas, E.S.E.I.A.A.T.-U.P.C., Colom 11, Terrassa,*
08222, Spain, e-mail: ramon.quintanilla@upc.edu

This paper presents a numerical study of the energetic behavior of some quasi-static thermoelastic problems in one- and two-dimensional settings. Firstly, we describe the two-dimensional thermoelastic problem decomposing the elastic tensor into two parts: the first one is positively defined for the first component of the displacement field, and the second one is negatively defined for the second component. The variational formulation is also derived. Restricting ourselves to the one-dimensional setting and assuming that the elastic coefficient is negative, we prove that the exponential energy decay follows if the coupling coefficient is smaller than the square root of the product between the heat capacity and the elastic coefficient. Then, fully discrete approximations are introduced by using the finite element method and the implicit Euler scheme. Some numerical simulations are performed: in a first one-dimensional example, we show the decay of the discrete energy depending on the value of the coupling coefficient and the heat diffusion. Secondly, two dimensional studies are considered depending on the expression of the elastic tensors, including diagonal matrices with the same eigenvalue, diagonal matrices with different eigenvalues and full matrices.

Key words: thermoelasticity without positive definite elasticity, exponential energy decay, finite elements, discrete energy decay, numerical simulations.

1. Introduction

The system of equations that governs thermoelastic deformations has been the subject of many studies, either in the nonlinear case or in the linearized case. In this paper, we analyze the linearized system. We can interpret this system by considering the small strains superimposed on a large strain [7, 11, 12, 18], but we restrict ourselves to the case where the temperature in the

equilibrium state is uniform. An existence theorem was obtained in [20] for the more general case when the temperature at the primary state is non-uniform. Throughout this work, we refer to the book by Ieşan and Scalia dedicated to the study of this type of problems [13].

It is well known that the usual system of thermoelasticity is rather complicated (see [2, Chapter 2] and [3, p. 311]). For this reason, there are several contributions for the case where the elasticity tensor is positively defined. However, when this condition is not satisfied, we are faced with an ill posed problem in Hadamard's sense, and although a uniqueness result can be obtained, the solutions can explode when time grows. Thus, in order to avoid several difficulties, some simplifications are required. A common modification is to consider the quasi-static problem. That is, we assume that the displacement is so slow that the acceleration is negligible. In this case, the system that describes the elastic deformations changes its nature, and we are faced with equations that can be elliptical [5, 6, 8, 9]. Over the last years, we have seen how the interest for the better understanding of quasi-static problems has restarted. It is worth recalling the contributions [14, 16], where the quasi-static approximation was justified for the isothermal elasticity in the case where the elasticity tensor was not necessarily positively defined. In isothermal viscoelasticity, Saccomandi and colleagues have examined quasi-static shearing motions in various cases (see [10, 21–23]). We can also cite the contribution [15], where the quasi-static approximation was justified for the thermoelasticity in the case where the elasticity tensor was assumed positively defined, or the work [1], where an approximate problem for the incremental thermoelasticity is analyzed from both the analytical and numerical points of view. A justification of the approach (as well as the result of the existence and uniqueness) in the case considered in this paper can be seen in the recent manuscript [17], where the authors have shown that the difference of the solutions between the dynamical and quasi-static problems can be controlled by a quantity related to the acceleration whenever a certain condition (satisfied in our case) holds.

The aim of this paper is to study numerically a couple of simple models for linearized thermoelasticity in the quasi-static case. Specifically, we study the one-dimensional problem when the elasticity coefficient is negative and the two-dimensional case assuming the elasticity tensor is positively defined with respect to one variable, but negatively defined with respect to the other variable. For this simplified one-dimensional case, we prove that, when the parameters fulfill a certain condition, the problem shows exponential decay for the temperature.

In the two-dimensional setting, we explore two different assumptions depending on the form of the elastic tensors: a simplified system with both elastic components decoupled and the coupled problem. This exploration is purely numerical, since the theoretical analysis cannot be extended to the multidimensional case.

We numerically show that, whenever the elasto-thermal coupling coefficient is small enough in comparison with the thermal capacity and the absolute value of the elasticity, the behavior of the solutions is exponentially stable. That is to say, the solutions tend to zero and this decay is controlled by a negative exponential. Certainly, this result is surprising in comparison with what happens in the dynamic case, where the solutions (as we have aforementioned) can explode. We conclude the two-dimensional studies considering the case where both elastic components are coupled with two more general cases: we first assume that the elasticity tensors are written as diagonal matrices (with different eigenvalues), and then that both matrices are full.

The outline of this paper is the following. In the next section, we describe the two-dimensional quasi-static thermoelastic problem that we simulate numerically later. We also show its one-dimensional version and we derive their variational formulations, which are written as coupled systems of first-order in time linear variational equations. Then, in Section 3, we introduce the numerical approximations by using the classical finite element method and the implicit Euler scheme. Finally, some numerical simulations involving one- and two-dimensional examples show the behavior of the discrete energy depending on the elastic tensors (their coefficients) and the heat diffusion. Several cases of these elastic tensors are considered assuming that they are diagonal (with the same or different eigenvalues) or full matrices.

2. The thermoelastic problems

Let us denote by Ω a bounded domain in $\mathbb{R}^2$, and let $[0, t_f]$ be the time interval of interest, with $t_f > 0$ being the final time. As usual in this type of analysis, let $\boldsymbol{x} = (x, y) \in \overline{\Omega}$ and $t \in [0, t_f]$ be the variables which represent space and time.

First, let us describe the thermomechanical problem. Let us denote by $\boldsymbol{u} = (u_1, u_2)$ the displacement field and by θ the temperature. Then, we consider the following problem:

$$(2.1) \qquad -\mu_{ij} u_{1,ij} + \beta\theta_{,1} = 0 \qquad \text{in} \quad \Omega \times (0, t_f),$$

$$(2.2) \qquad -\mu^*_{ij} u_{2,ij} + \beta\theta_{,2} = 0 \qquad \text{in} \quad \Omega \times (0, t_f),$$

$$(2.3) \qquad c\dot{\theta} = \kappa\Delta\theta - \beta(\dot{u}_{1,1} + \dot{u}_{2,2}) \quad \text{in} \quad \Omega \times (0, t_f),$$

$$(2.4) \qquad u_1 = u_2 = \theta = 0 \qquad \text{on} \quad \partial\Omega \times (0, t_f),$$

$$(2.5) \qquad \theta(\boldsymbol{x}, 0) = \theta^0(\boldsymbol{x}) \qquad \text{for a.e. } \boldsymbol{x} \in \Omega.$$

In the previous system of equations, (μ_{ij}) and (μ^*_{ij}) represent the elasticity tensors for each component of the displacements, $c > 0$ is the heat capacity,

κ is the thermal diffusion and $\beta \neq 0$ is the coupling coefficient that we assume is small enough. For the sake of simplicity in the analysis presented in the next sections, we have assumed that both components of the displacements are uncoupled and so, the elasticity tensor can be defined separately for each of them. In order to define our problem, we assume that tensor (μ_{ij}) is positively defined and that tensor (μ_{ij}^*) is negatively definite.

REMARK 1. We note that, even if the aim of this study is to consider this thermomechanical problem from the mathematical point of view, this type of materials can be obtained when the elasticity tensors are anisotropic. As an example, we assume that

$$d_{ijkl} = C_{ijkl} + \tau_{jl}\delta_{ik},$$

where d_{ijkl} is the prestressed elasticity tensor, C_{ijkl} is the usual elasticity tensor and τ_{jl} are the prestresses.

In this case, we can use the following conditions:

$$C_{1111} + \tau_{11} = \mu_{11}, \quad \tau_{22} = \mu_{22}, \quad \tau_{12} = \mu_{12},$$
$$C_{2222} + \tau_{22} = \mu_{22}^*, \quad \tau_{11} = \mu_{11}^*, \quad \tau_{12} = \mu_{12}^*,$$

and the other coefficients C_{ijkl} vanish.

Since μ_{ij} is assumed to be positively defined, it is equivalent to impose that

$$(2.6) \qquad C_{1111} + \tau_{11} > 0, \quad \tau_{22}(C_{1111} + \tau_{11}) > \tau_{12}^2,$$

and, similarly, the fact that μ_{ij}^* is negatively defined means that:

$$(2.7) \qquad C_{2222} + \tau_{22} < 0, \quad \tau_{11}(C_{2222} + \tau_{22}) > \tau_{12}^2.$$

We note that conditions (2.6) and (2.7) are compatible for a suitable choice of the parameters. For instance, we can select C_{1111} positive and τ_{11} negative with

$$C_{1111} > -\tau_{11},$$

and C_{2222} negative and τ_{22} positive such that

$$C_{2222} < -\tau_{22}.$$

The second condition in (2.6) can be written as

$$\tau_{22}C_{1111} > -\tau_{11}\tau_{22} + \tau_{12}^2,$$

and the second condition in (2.7) as

$$\tau_{11}C_{2222} > -\tau_{11}\tau_{22} + \tau_{12}^2.$$

We note that these conditions would be satisfied whenever C_{1111} and $-C_{2222}$ are large enough in comparison with $-\tau_{11}$, τ_{12} and τ_{22}. Moreover, we also point out that, in the case of the linearized elasticity, we could choose the coefficients in a weaker way.

Now, we obtain the variational formulation of the problem. So, let us denote by $Y = L^2(\Omega)$, $H = [L^2(\Omega)]^2$ and $V = H_0^1(\Omega)$. Multiplying Eqs. (2.1)–(2.3) by adequate test functions and using boundary conditions (2.4), we have the following weak form of the problem (2.1)–(2.5).

Find the first component of the displacements $u_1 : [0, t_f] \to V$, the second component of the displacements $u_2 : [0, t_f] \to V$ and the temperature $\theta : [0, t_f] \to V$ such that $\theta(0) = \theta^0$, and for a.e. $t \in (0, t_f)$ and for all $w, r, z \in V$,

$$(2.8) \qquad 2(\mu_{ij} u_{1,i}(t), w_{,j})_Y + \beta(\theta_{,1}(t), w)_Y = 0,$$

$$(2.9) \qquad (\mu_{ij}^* u_{2,i}(t), r_{,j})_Y + \beta(\theta_{,2}(t), r)_Y = 0,$$

$$(2.10) \qquad c(\dot{\theta}(t), z)_Y + \kappa(\nabla\theta(t), \nabla z)_H + \beta(\dot{u}_{1,1}(t) + \dot{u}_{2,2}(t), z)_Y = 0.$$

2.1. The one-dimensional setting

Since we consider a simpler problem involving the one-dimensional setting in the section describing the numerical results, we present it below. First, we assume that $\Omega = (0, 1)$ and we solve the following system:

$$(2.11) \qquad -\mu^* u_{xx} - \beta\theta_x = 0 \quad \text{in} \quad (0, 1) \times (0, t_f),$$

$$(2.12) \qquad c\dot{\theta} = \kappa\theta_{xx} - \beta\dot{u}_x \quad \text{in} \quad (0, 1) \times (0, t_f),$$

$$(2.13) \qquad u(x, t) = \theta(x, t) = 0 \quad \text{for } x = 0, 1, \ t \in (0, t_f),$$

$$(2.14) \qquad \theta(x, 0) = \theta^0(x) \qquad \text{for a.e. } x \in (0, 1).$$

In this system, we have assumed that $\mu_{11}^* = -\mu^*$, where μ^* is positive. After taking into account the boundary conditions (2.13) and integrating Eq. (2.11) with respect to x, we find that

$$\mu^* u_x(x, t) = \mu^* u_x(0, t) - \beta\theta(x, t).$$

If we integrate it once again, it leads to

$$\mu^* u(x, t) = \mu^* x u_x(0, t) - \beta \int_0^x \theta(\xi, t) \, d\xi,$$

but, since $u(1, t) = 0$ for all $t \in (0, t_f)$, we obtain

$$0 = \mu^* u_x(0, t) - \beta \int_0^1 \theta(\xi, t) \, d\xi \to u_x(0, t) = \frac{\beta}{\mu^*} \int_0^1 \theta(\xi, t) \, d\xi.$$

Thus, we have

$$\dot{u}_x(x,t) = \dot{u}_x(0,t) - \frac{\beta}{\mu^*}\dot{\theta}(x,t) = \frac{\beta}{\mu^*}\int_0^1 \dot{\theta}(\xi,t)\,d\xi - \frac{\beta}{\mu^*}\dot{\theta}(x,t),$$

and Eq. (2.12) is written as

$$\left(c - \frac{\beta^2}{\mu^*}\right)\dot{\theta} = \kappa\theta_{xx} - \frac{\beta^2}{\mu^*}\int_0^1 \dot{\theta}(\xi,t)\,d\xi.$$

If we consider the auxiliary function

$$F(t) = \left(c - \frac{\beta^2}{\mu^*}\right)\int_0^1 \theta^2\,dx + \frac{\beta^2}{\mu^*}\left(\int_0^1 \theta(\xi,t)\,d\xi\right)^2,$$

we can easily show that

$$\dot{F}(t) = -2\kappa\int_0^1 \kappa|\theta_x|^2\,dx.$$

Keeping in mind that

$$\left(\int_0^1 \theta(\xi,t)\,d\xi\right)^2 \leq \int_0^1 \theta^2(\xi,t)\,d\xi,$$

we conclude that there is an exponential decay for the temperature when $c\mu^* > \beta^2$. In this case, the "limit value" could be $|\beta| = \sqrt{c\mu^*}$.

Then, we have obtained that

$$F(t) \leq F(0)e^{-\omega t},$$

where ω is a positive constant. Now, if we define the function

$$G(t) = \int_0^1 u_x^2\,dx,$$

from Eq. (2.11) and boundary conditions (2.13) we see that

$$\mu^*\int_0^1 u_x^2\,dx + \beta\int_0^1 \theta u_x\,dx = 0.$$

Thus, we find that

$$G(t) \leq \frac{|\beta|}{\mu^*} \left(\int_0^1 \theta^2 \, dx \right)^{1/2} G(t)^{1/2}.$$

It then follows that

$$G(t) \leq \frac{\beta^2}{|\mu^*|^2} F(0) e^{-\omega t}.$$

The above estimates on F and G lead to the exponential decay of the solutions to the problem (2.11)–(2.14).

Now, we derive the corresponding variational formulation of the problem (2.11)–(2.14), which is written as follows:

Find the displacement $u : [0, t_f] \to V$ and the temperature $\theta : [0, t_f] \to V$ such that $\theta(0) = \theta^0$, and for a.e. $t \in (0, t_f)$ and for all $w, z \in V$,

(2.15) $$\mu^*(u_x(t), w_x)_Y - \beta(\theta_x(t), w)_Y = 0,$$

(2.16) $$c(\dot{\theta}(t), z)_Y + \kappa(\theta_x(t), z_x)_Y + \beta(\dot{u}_x(t), z)_Y = 0.$$

3. Fully discrete approximations

In this section, we introduce a finite element algorithm for approximating solutions to the variational problem (2.8)–(2.10). This is done in two steps. First, we construct the finite element space V^h to approximate the variational space V given by

(3.1) $$V^h = \{z^h \in C(\overline{\Omega}) \; ; \; z^h_{|Tr} \in P_1(Tr) \, \forall Tr \in \mathcal{T}^h, \; z^h = 0 \text{ on } \partial\Omega\},$$

where $\overline{\Omega}$ is assumed to be a polyhedral domain, $\mathcal{T}^h$ denotes a triangulation of $\overline{\Omega}$, and $P_1(Tr)$ represents the space of polynomials of global degree less than or equal to 1 in Tr, i.e. the variational space V is approximated by continuous and piecewise linear finite elements. Here, $h > 0$ denotes the spatial discretization parameter.

Secondly, the time derivatives are discretized by using a uniform partition of the time interval $[0, t_f]$, denoted by $0 = t_0 < t_1 < \cdots < t_N = t_f$, and let k be the time step size, $k = t_f/N$. Moreover, for a sequence $\{z_n\}_{n=0}^N$, let $\delta z_n = (z_n - z_{n-1})/k$ be the divided differences.

Using the well-known backward Euler scheme for the discretization of the time derivatives, the fully discrete approximation of problem (2.8)–(2.10) is the following:

Find the first component of the discrete displacements $\{u_{1n}^{hk}\}_{n=0}^N \subset V^h$, the second component of the discrete displacements $\{u_{2n}^{hk}\}_{n=0}^N \subset V^h$ and the discrete

temperature $\{\theta_n^{hk}\}_{n=0}^N \subset V^h$ *such that* $\theta_0^{hk} = \theta^{0h}$, *and for* $n = 1, \ldots, N$, *and for all* $w^h, r^h, z^h \in V^h$,

(3.2) $$(\mu_{ij} u_{1n,i}^{hk}, w_{,j}^h)_Y + \beta(\theta_{n,1}^{hk}, w^h)_Y = 0,$$

(3.3) $$(\mu_{ij}^* u_{2n,i}^{hk}, r_{,j}^h)_Y + \beta(\theta_{n,2}^{hk}, r^h)_Y = 0,$$

(3.4) $$c(\delta\theta_n^{hk}, z^h)_Y + \kappa(\nabla\theta_n^{hk}, \nabla z^h)_H + \beta(\delta u_{1n,1}^{hk} + \delta u_{2n,2}^{hk}, z^h)_Y = 0.$$

Here, θ^{0h} is the approximation of the initial condition θ^0 defined as

$$\theta^{0h} = \mathcal{P}^h \theta^0,$$

where $\mathcal{P}^h$ is the classical finite element interpolation operator over V^h (see, e.g., [4]). Regarding the "artificial" discrete initial conditions for the two components of the displacements, u_{10}^{hk} and u_{20}^{hk} respectively, they are obtained solving the following equations, for all $w^h, r^h \in V^h$,

$$(\mu_{ij} u_{10,i}^{hk}, w_{,j}^h)_Y + \beta(\theta_{,1}^{0h}, w^h)_Y = 0,$$
$$(\mu_{ij}^* u_{20,i}^{hk}, r_{,j}^h)_Y + \beta(\theta_{,2}^{0h}, r^h)_Y = 0.$$

We use the classical Lax–Milgram lemma to prove that the discrete problem (3.2)–(3.4) has a unique solution. Thus, we define the bilinear form A given by:

$$A(\boldsymbol{u}_n^{hk}, \boldsymbol{v}^h) = (\mu_{ij} u_{1n,i}^{hk}, w_{,j}^h)_Y + (\mu_{ij}^* u_{2n,i}^{hk}, r_{,j}^h)_Y + \beta(\theta_{n,1}^{hk}, w^h)_Y + \beta(\theta_{n,2}^{hk}, r^h)_Y$$
$$+ c(\theta_n^{hk}, z^h)_Y + \kappa k(\nabla\theta_n^{hk}, \nabla z^h)_H + \beta(u_{1n,1}^{hk} + u_{2n,2}^{hk}, z^h)_Y,$$

where $\boldsymbol{u}_n^{hk} = (u_{1n}^{hk}, u_{2n}^{hk}, \theta_n^{hk}) \in V^h \times V^h \times V^h$ and $\boldsymbol{v}^h = (w^h, r^h, z^h) \in V^h \times V^h \times V^h$ and the linear form L defined as

$$L(\boldsymbol{z}^h) = c(\theta_{n-1}^{hk}, z^h)_Y + \beta(u_{1n-1,1}^{hk} + u_{2n-1,2}^{hk}, z^h)_Y.$$

Therefore, the problem (3.2)–(3.4) leads to the equation

$$A(\boldsymbol{u}_n^{hk}, \boldsymbol{v}^h) = L(\boldsymbol{v}^h) \quad \forall \boldsymbol{v}^h \in V^h \times V^h \times V^h.$$

Thanks to the assumptions stated in the previous sections, we could easily prove that the bilinear form A is coercive, and a direct application of the Lax–Milgram lemma allows us to conclude that the discrete problem has a unique solution.

REMARK 2. We note that, proceeding as in other contributions, we could develop the numerical analysis of problem (2.8)–(2.10) approximated by fully discrete problem (3.2)–(3.4). Indeed, we could obtain some a priori error estimates as we did in [1]. The key point is that we have written variational equations (2.9) and (3.3) changing the sign of the coupling coefficient β. Therefore, the estimates of function u_2 could be obtained following the estimates of function u_1.

REMARK 3. Again, we present the numerical approximation of the one-dimensional problem (2.15) and (2.16).

Proceeding in a similar form as for the two-dimensional setting, we have the following discrete problem.

Find the discrete displacements $\{u_n^{hk}\}_{n=0}^N \subset V^h$ *and the discrete temperature* $\{\theta_n^{hk}\}_{n=0}^N \subset V^h$ *such that* $\theta_0^{hk} = \theta^{0h}$, *and for* $n = 1, \ldots, N$ *and for all* $w^h, z^h \in V^h$,

$$(3.5) \qquad \mu^*((u_n^{hk})_x, w_x^h)_Y - \beta((\theta_n^{hk})_x, w^h)_Y = 0,$$

$$(3.6) \qquad c(\delta\theta_n^{hk}, z^h)_Y + \kappa((\theta_n^{hk})_x, z_x^h)_Y + \beta((\delta u_n^{hk})_x, z^h)_Y = 0,$$

where the "artificial" initial condition for the displacements, u_0^{hk}, is obtained solving the following discrete variational equation:

$$\mu^*((u_0^{hk})_x, w_x^h)_Y - \beta((\theta^{0h})_x, w^h)_Y = 0.$$

4. Numerical results

The numerical problem was solved using FEniCS [19] in a 4 core 3.40 GHz computer with 16 GB of RAM, where a typical two-dimensional run with 20 elements and 10000 timesteps takes around 65 seconds.

Following [17], we consider the energy of the system given by

$$E(t) = \frac{1}{2} \int_\Omega \theta^2(\boldsymbol{x}, t) \, dv.$$

We divide the studies in two sections: the one-dimensional problems and the two-dimensional ones. For the one-dimensional cases, we first check how the energy decay depends on the coupling coefficient β and on the diffusion parameter κ. The two-dimensional studies are subdivided into two subsections. In the first one, the elasticity tensors have two equal eigenvalues, providing a framework that is more comparable to the one-dimensional case. For that case, we explore the influence of the timestep, and the parameters μ and μ^*. In the second subsection, we consider the general case where the eigenvalues of the elasticity tensors are distinct. Here, we look for a relationship between β_{lim} and the eigenvalues of such tensors.

4.1. One-dimensional studies

In the one-dimensional setting, it is possible to analytically find the limit value for β that causes the model's energy to decrease; we call this value β_{lim}.

As shown in Section 2.1, the following condition must be met for the model to exhibit the exponential energy decay:

$$|\beta_{lim}| < \sqrt{c \cdot \mu^*}.$$

To check how the energy depends on β, we perform a numerical experiment varying this parameter ($\beta \in [1,2]$) and fixing all the other parameters with the following values:

$$\mu^* = 10, \quad c = 7, \quad \kappa = 5.$$

The initial condition for the temperature θ is $\theta^0(x) = 1000\, x^2\, (x-1)^2$ for $x \in (0,1)$. We run the simulation until $t_f = 1$ with a timestep of $k = 10^{-5}$ and 20 elements to discretize the spatial domain $\Omega = (0,1)$ (which results in $h = 0.05$); we ensured that both discretization parameters were fine enough to obtain consistent results.

The results show that energy decay in the one-dimensional model is exponential independently of the value of β; as long as it verifies the previous condition. This can be clearly seen in Fig. 1, where the energy is plotted in a semilogarithmic graph for different values of β; the linear graph in the semi-log plot shows the mentioned exponential decay.
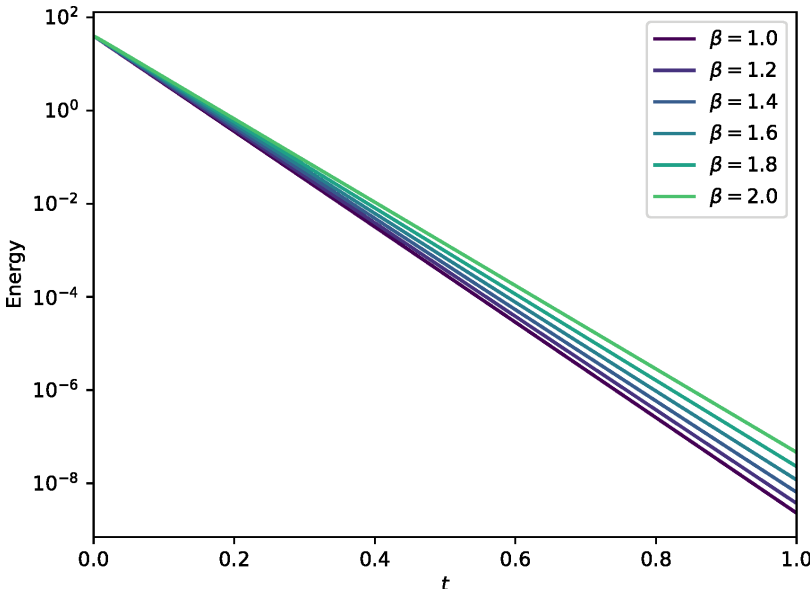

Fig. 1. Energy decay of the system in a semilogarithmic plot for different values of β. The straight lines in the semi-log plot indicate that the decay is exponential.

4.1.1. Influence of κ. Although β_{lim} should not depend on κ, according to the theoretical analysis, we found a "numerical" dependence on this parameter. Higher values of κ yielded values for β_{lim} higher than expected. The explanation for this effect became clear when we studied the dependency of β_{lim} with the timestep k. For this experiment we took the following parameters:

$$c = 0.5, \quad \mu^* = 100,$$

resulting in a $\beta_{lim} = 7.071$. The initial condition and discretization values are the same as before.

We performed a parametric study for several values for κ; for each value we computed the limit value for β using a bisection algorithm in the neighbourhood of the theoretical value for β_{lim}. After repeating such a study for different timesteps, we found that κ influenced the timestep required to capture β_{lim} properly. The results of the parametric study are plotted in Fig. 2. They indicate that as κ increases, a finer timestep is required to find a limit value closer to the theoretical value (plotted as a horizontal line in red).
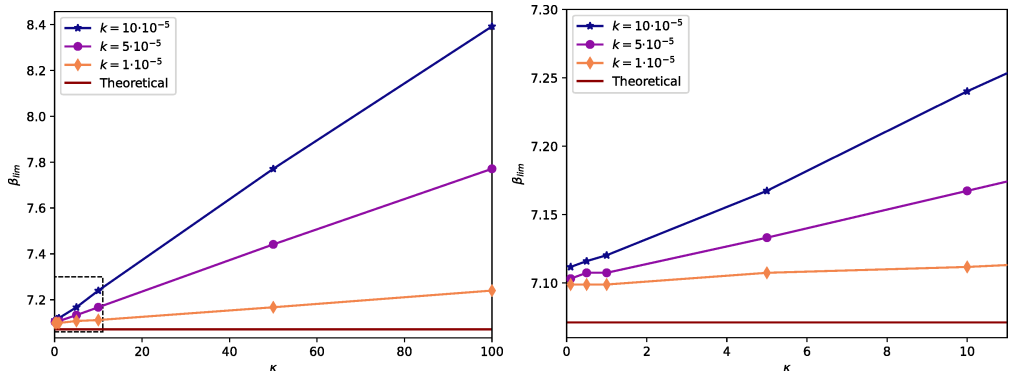

Fig. 2. Limit value for β computed for different κ and timesteps. The horizontal red line represents the theoretical value, which should be independent of κ. The plot on the right shows a zommed-in version of the left plot.

4.2. Two-dimensional studies

In this subsection, we present some two-dimensional numerical simulations assuming that the elasticity tensors have different forms.

We start considering diagonal elasticity tensors with the same eigenvalues, which means that both elasticity components are decoupled. Then, we continue extending the above case assuming that the eigenvalues are different and, finally, that the matrices defining the elastic tensors are full.

4.2.1. First $2D$-example: numerical limit for β and explosion of the energy with diagonal elasticity tensors. In this two-dimensional problem, we found numerically that a limit value for β is also present. In this case, we expect cases with a value of β above the limit to result in an uncontrolled energy increase with time. To investigate this effect numerically, we perform an experiment in a two-dimensional square domain $\Omega = (0,1) \times (0,1)$. The spatial discretization is performed with a mapped mesh of quadrilateral elements (20 elements in each side of the square). To investigate the effect of the temporal discretization, we repeat the simulations with different timesteps.

In the examples provided in this case, we assume that the elasticity tensors correspond to diagonal matrices with the same eigenvalues, that is, we take the tensors $\mu_{ij} = \mu \delta_{ij}$ and $\mu_{ij}^* = -\mu^* \delta_{ij}$, where $\mu, \mu^* \in \mathbb{R}^+$ and δ_{ij} represents the Kronecker symbol.

The model parameters are the following:

$$\mu = 10, \quad \mu^* = 10, \quad c = 7, \quad \kappa = 5.$$

The initial condition for the two-dimensional problem is an extension of the one-dimensional one:

$$(4.1) \qquad \theta^0(x,y) = 1000x^2(x-1)^2y^2(y-1)^2 \quad \forall (x,y) \in (0,1) \times (0,1).$$

To explore the influence of the timestep, we experiment with two values of β: one slightly above the limit value and the other slightly below. Numerically, we find that the limit value for β is between 8.917 and 8.928, so those are the values considered for the study. We note that, if we use the calculation of the one-dimensional case, the limit value would be $\beta_{lim} = 8.367$. Then, we vary the timestep ($k = 5 \cdot 10^{-7}$ being the finest) for both values of β to investigate its effect.

In Fig. 3, we plot the energy for two different values of β (the previously mentioned values 8.917 and 8.928), and four different values of the timestep. We can see that the timestep does not affect the cases with the exponential energy decay, but it dramatically affects the ones where the energy increases. With bigger timesteps (a more coarse simulation) the energy is numerically damped, and the simulation takes longer to explode (exponential growth of the energy); however, this effect is purely numerical, since refining the timestep yields a solution that explodes faster. This effect can be seen more clearly in the right figure, where a zoom around the origin was made.

Since in the two-dimensional case a new parameter (μ) appears, we asked ourselves what kind of effect it had in the exponential energy decay. Although theoretically it should not have any effect in the energy behavior of the model, we have previously discussed that the diffusion parameter κ had an effect in
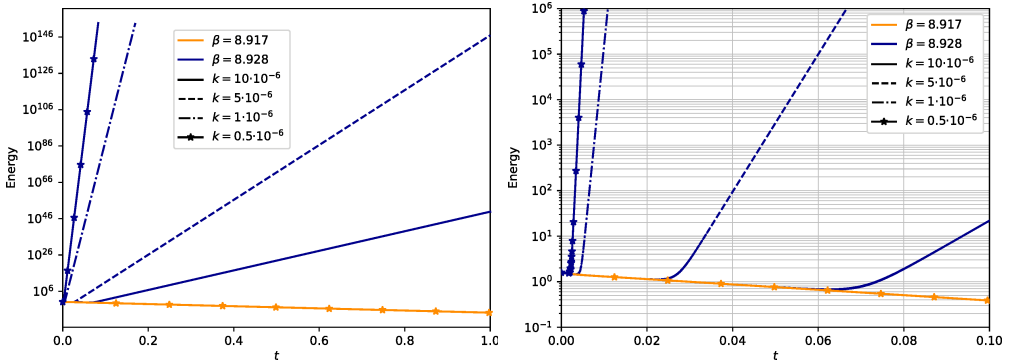
FIG. 3. Energy decay for two different values of β (one results in an exponential energy decay and the other one in the explosion of the energy) studied with different timesteps. A zoom near the origin is enhanced in the right figure.

the timestep, which resulted in deviations from the theoretical condition for the exponential energy decay. The parameters for this experiment are the following:

$$\beta = 0.1, \qquad \mu^* = 10, \qquad c = 10, \qquad \kappa = 5,$$

keeping the same discretization parameters as before ($h = 0.05$, $k = 10^{-5}$).

In this case, after obtaining some results, we found that μ had no effect in the decay rate of the energy nor in the condition for the exponential energy decay. This is shown in Fig. 4, where a wide range of values for μ were simulated, yielding in all cases the same decay rate (with no increasing of the energy).
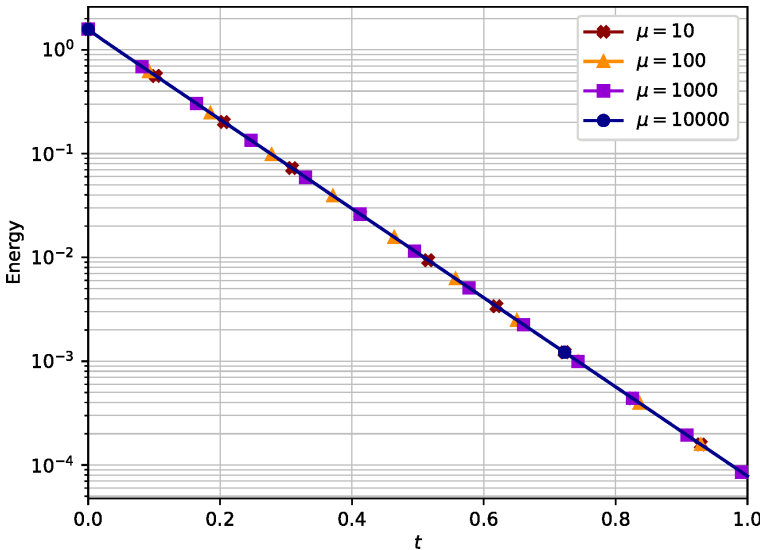

FIG. 4. Energy decay for different values of μ represented in a semilogarithmic plot. The straight line indicates the decay is exponential and, since all the lines match, independent of μ.

To finish these first numerical experiments, we analyze the effect of μ^* fixing all the other parameters:

$$\beta = 10, \quad \mu = 10, \quad c = 10, \quad \kappa = 5.$$

We keep the same discretization and initial condition as before.

In Fig. 5, we show the energy decay for some values of μ^*. We recall that, in order to fulfil the condition for the exponential energy decay, the value of the parameter must be above some limit value; in this case 10. We can see that the decay is exponential, and the decay rate decreases rapidly as the parameter increases. This relationship appears more clearly in the right figure, where the rate of the exponential is plotted against μ^*. This exponent appears to converge to a limit value plotted in red (this limit value was computed for $\mu^* = 10^4$).
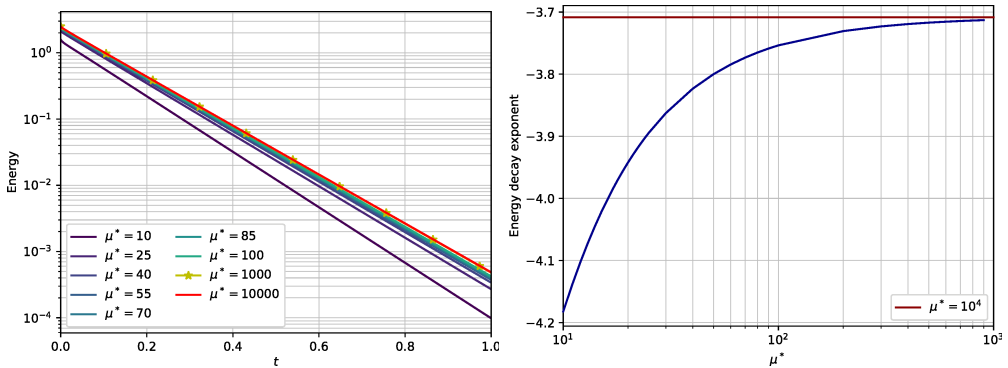

FIG. 5. Left: energy decay for different values of μ^* represented in a semilogarithmic plot; all cases present exponential decay. Right: exponent of the decay represented as a function of μ^*; the horizontal axis is logarithmic. The decay rate converges to an asymptotic value.

4.2.2. Comparative of different elasticity tensors. Up to this point, the elasticity tensors were considered diagonal with both values on the diagonal equal. In this section, we study what properties of the elasticity tensors influence the limit value of beta. Hence, we define two different cases: diagonal tensors with two distinct values and two full tensors. In both cases, the tensors have the same eigenvalues, choosing the following distinct eigenvalues: 7 and 2; 70 and 20 for μ_{ij} and -7 and -2; -70 and -20 for μ_{ij}^*. The matrices considered for eigenvalues 7 and 2, and 70 and 20 are:

$$\begin{pmatrix} 5 & 3 \\ 2 & 4 \end{pmatrix}, \quad \begin{pmatrix} 80 & \sqrt{600} \\ -\sqrt{600} & 10 \end{pmatrix},$$

and the ones considered for eigenvalues -7 and -2, and -70 and -20 are:

$$\begin{pmatrix} -8 & 2 \\ -3 & -1 \end{pmatrix}, \quad \begin{pmatrix} -50 & \sqrt{600} \\ \sqrt{600} & -40 \end{pmatrix}.$$

The other model parameters are $c = 10$ and $\kappa = 5$. The simulations were performed with 20 by 20 elements and a timestep of 10^{-6}; we also did a sensitivity analysis to assure the results were not dependent on the mesh size and timestep. The initial condition is the same as before, see (4.1).

For each tensor type and eigenvalue combination, we compute the limit value for β; the results obtained are summarized in Table 1 for the diagonal tensors and Table 2 for the complete tensors. The results indicate that μ_{ij} has, in general, a negligible effect in β_{lim}, as shown in the previous examples; however, μ_{ij}^* has a much bigger impact in the stability of the problem. Comparing the cases with the diagonal and full matrices, we cannot conclude that the limit value of β depends exclusively on the eigenvalues, because the value of β_{lim} changes even for matrices with the same eigenvalues; further research is required to find which properties of the tensors determine this factor.

TABLE 1. Limit values for β for different diagonal elasticity tensors.

eig(μ_{ij})	eig(μ_{ij}^*)	β_{lim}
7, 2	$-7, -2$	4.93
70, 20	$-7, -2$	4.94
7, 2	$-70, -20$	16.19
70, 20	$-70, -20$	16.21

TABLE 2. Limit values for β for different complete elasticity tensors.

eig(μ_{ij})	eig(μ_{ij}^*)	β_{lim}
7, 2	$-7, -2$	3.58
70, 20	$-7, -2$	3.57
7, 2	$-70, -20$	21.62
70, 20	$-70, -20$	20.01

Finally, we set a fixed $\beta = 3.5$ for all cases, below the minimum β_{lim} we obtained, in order to have a stable model. With this setup, we compute the energy in order to assess the decay rate. The results are shown in Fig. 6. All the simulations show the exponential decay. The decay rates are different in general, but we note that in the cases where eig$(\mu_{ij}) = -$eig(μ_{ij}^*) (when eig$(\mu_{ij}) = (7, 2)$; eig$(\mu_{ij}^*) = (-7, -2)$ and eig$(\mu_{ij}) = (70, 20)$; eig$(\mu_{ij}^*) = (-70, -20)$) the decay rates are almost equal.

As a possible conclusion of the above studies, we could say that the limit value of β is not directly related to the eigenvalues of these elastic tensors.
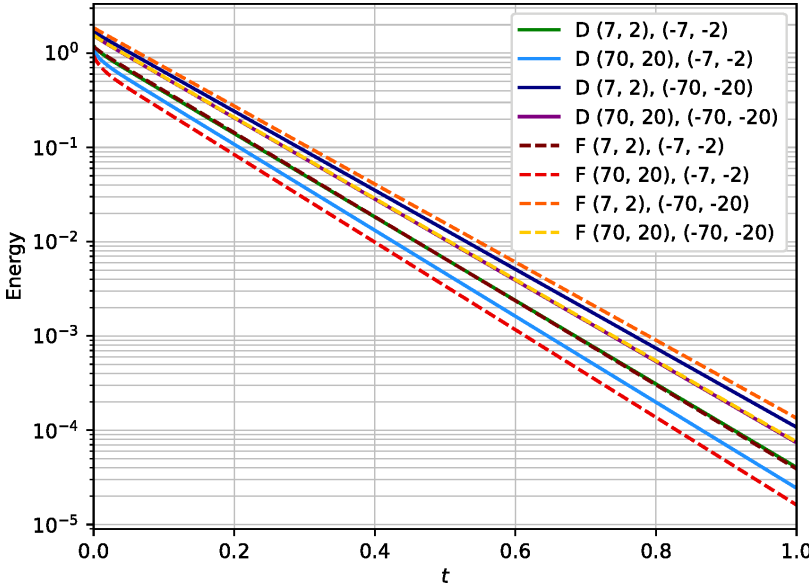
Fig. 6. Energy decay for all the cases presented in this section. In solid line with cold colors (marked with D in the legend) the cases with diagonal elasticity tensors. In dashed lines with warm colors (marked with F in the legend) the cases with complete elasticity tensors. The eigenvalues of μ_{ij} and μ_{ij}^* are listed in the legend between brackets.

Conclusions

In this paper, we have studied the energetic behavior of some quasi-static thermoelastic problems assuming that the elastic tensor (or one of its parts) is not positively defined. For the one-dimensional case, we have obtained a condition among the thermal coupling coefficient β and the product of the heat capacity c and the elastic coefficient μ^*. Then, we have introduced fully discrete approximations by using the finite element method and the implicit Euler scheme to approximate the spatial variable and to discretize the time derivatives, respectively. Finally, we have shown some numerical simulations. The first ones include one-dimensional examples, demonstrating the commented condition on the constitutive coefficients and the influence of the parameters β and κ. The second numerical simulations depend on the form of the elasticity coefficients, assuming that the elastic tensors are diagonal (with the same or different eigenvalues) or full matrices. In the latter case, we cannot conclude any relation among the eigenvalues.

References

1. N. BAZARRA, J.R. FERNÁNDEZ, R. QUINTANILLA, *On the approximate problem for the incremental thermoelasticity*, Journal of Thermal Stresses, **44**, 619–633, 2021.

2. B.A. BOLEY, J.H. WEINER, *Theory of Thermal Stresses*, John Wiley, New York, 1960.

3. D.E. CARLSON, Linear thermoelasticity, Flugge Handbuch der Physik, Vol VI a/2 (ed. C. Truesdell), Springer, Berlin, 297–345, 1972.

4. P.G. CIARLET, *Basic error estimates for elliptic problems*, [in:] *Handbook of Numerical Analysis*, P.G. Ciarlet and J.L. Lions [eds.], 17–351, 1993.

5. W.A. DAY, *Justification of the uncoupled and quasi-static approximation in the problem of dynamic thermoelasticity*, Archive for Rational Mechanics and Analysis, **77**, 387–396, 1981.

6. W.A. DAY, *Further justification of the uncoupled and quasi-approximations in thermoelasticity*, Archive for Rational Mechanics and Analysis, **79**, 85–95, 1982.

7. A.H. ENGLAND, A.E. GREEN, *Steady-state thermoelasticity for initially stressed bodies*, Philosophical Transactions of the Royal Society of London Series A, Mathematical and Physical Sciences, **253**, 517–542, 1961.

8. B.F. ESHAM, R.J. WEINACHT, *Singular perturbations and the coupled/quasi-static approximation in linear thermoelasticity*, SIAM Journal on Mathematical Analysis, **25**, 1521–1536, 1994.

9. B.F. ESHAM, R.J. WEINACHT, *Limitation of the coupled/quasi-static approximation in multi-dimensional linear thermoelasticity*, Applicable Analysis, **73**, 72–87, 1999.

10. M.D. GILCHRIST, B. RASHID, J.G. MURPHY, G. SACCOMANDI, *Quasi-static deformations of biological soft tissue*, Mathematics and Mechanics of Solids, **18**, 6, 622–633, 2013.

11. A.E. GREEN, *Thermoelastic stresses in initially stressed bodies*, Proceedings of the Royal Society of London A, **266**, 119, 1962.

12. D. IEŞAN, *Incremental equations in thermoelasticity*, Journal of Thermal Stresses, **3**, 41–56, 1980.

13. D. IEŞAN, A. SCALIA, *Thermoelastic Deformations*, Kluwer Academic Publishers, Dordrecht, 1996.

14. R.J. KNOPS, *On the Quasi-Static Approximation to the Initial Traction Boundary Problem of Linear Elastodynamics*, [in:] New Achievements in Continuum Mechanics and Thermodynamics, B.E. Abali *et al.* [eds.], Advanced Structured Materials, **108**, Springer Nature, Switzerland, 2019.

15. R.J. KNOPS, R. QUINTANILLA, *On quasi-static approximations in linear thermoelastodynamics*, Journal of Thermal Stresses, **41**, 1432–1449, 2018.

16. R.J. KNOPS, R. QUINTANILLA, *On the quasi-static approximation in the initial boundary value problem of linearised elastodynamics*, Journal of Engineering Mathematics, **126**, 11, 2021.

17. R.J. KNOPS, R. QUINTANILLA, *On existence and uniqueness for a quasi-static thermoelastic problem*, in preparation, 2023.

18. R.J. Knops, E.W. Wilkes, *Theory of elastic stability*, Flugge Handbuch der Physik, Vol VI a/3, C. Truesdell [ed.], Springer Verlag, Berlin, 125–302, 1973.

19. A. Logg, K.-A. Mardal, G. Wells, *Automated Solution of Differential Equations by the Finite Element Method*, Springer, 2012.

20. C.B. Navarro, R. Quintanilla, *On existence and uniqueness in incremental thermoelasticity*, Zeitschrift füe Angewandte Mathematik und Physik, **35**, 206–215, 1984.

21. E. Pucci, G. Saccomandi, *On a special class of nonlinear viscoelastic solids*, Mathematics and Mechanics of Solids, **15**, 803–811, 2010.

22. E. Pucci, G. Saccomandi, *On the nonlinear theory of viscoelasticity of differential type*, Mathematics and Mechanics of Solids, **17**, 624–630, 2012.

23. G. Saccomandi, L. Vergori, *Large time approximation for shearing motions*, SIAM Journal of Applied Mathematics, **78**, 1964–1983, 2016.